0026-895X/94/020313-10$03.00/0

MOLECULAR PHARMACOLOGY, 46:313–322, 1994.

Sequence-selective Binding to DNA of *Cis*- and *Trans*-butamidine Analogues of the Anti-*Pneumocystis Carinii* Pneumonia Drug Pentamidine

CHRISTIAN BAILLY,[1] ISAAC O. DONKOR, DEAN GENTLE, MARTIN THORNALLEY, and MICHAEL J. WARING

Department of Pharmacology, University of Cambridge, Cambridge CB2 1QJ, UK (C.B., D.G., M.T., M.J.W.), and College of Pharmacy, University of Tennessee Health Science Center, Memphis, Tennessee 38163 (I.O.D.)

Received February 25, 1994; Accepted May 18, 1994

SUMMARY

Footprinting experiments using both DNase I and methidium propyl-EDTA·Fe(II) have been used to investigate the sequence selectivity in binding to DNA of pentamidine and four butamidine analogues active against the *Pneumocystis carinii* pathogen, which afflicts patients with acquired immunodeficiency syndrome. In common with pentamidine, the butamidine drugs, which contain *cis*- or *trans*-1,4-but-2-ene linkers and either bis(amidine) or bis(imidazolidine) terminal groups, bind selectively to DNA sequences composed of at least 4 consecutive A·T base pairs. None of the drugs tolerates the presence of a G·C base pair within the binding site. Consistently in the DNase I and methidium propyl-EDTA·Fe(II) footprinting experiments, the *cis*-isomers produce stronger footprints than do the *trans*-isomers, despite their similar hydrogen-bonding potentialities. The present experimental data support the view that the conformation of the drug plays a determining role in the binding reaction. Starting from the known structure of a pentamidine-oligonucleotide complex, it is possible to rationalize the different capacities of the *cis*- and *trans*-butamidine analogues to recognize defined DNA sequences in terms of the radius of curvature of the molecule and the distance between the positively charged terminal groups. Together, these features constitute critical factors favoring (*cis*-conformation) or hampering (*trans*-conformation) the fitting of the drugs into the minor groove of DNA. In terms of structure-activity relationships, the AT-specific recognition of DNA by this series of butamidine derivatives cannot be directly correlated with their potencies against *Pneumocystis carinii* pneumonia.

Pentamidine is a bis-amidine aromatic compound (Fig. 1) that is widely used clinically for the treatment of PCP in patients with acquired immunodeficiency syndrome (1–3). The pharmacological importance of the drug has greatly increased over the last few years due to the inexorable spread of acquired immunodeficiency syndrome (4). Despite its effectiveness, the use of pentamidine is associated with severe adverse effects, which limit its use. Accordingly, the design of more effective and less toxic analogues is a matter of vital research interest.

Direct interaction with nucleic acids is thought to be central to the molecular mechanism by which pentamidine acts (5). The structure of a pentamidine-oligonucleotide complex has been determined by X-ray crystallography to atomic resolution (6). The interaction of pentamidine with DNA has also been explored recently by two-dimensional NMR spectroscopy (7), footprinting (8), and molecular modeling analyses (9, 10). All of these studies converge to show that the drug binds preferentially to the minor groove of DNA at AT-rich sequences, in a manner analogous to that observed with the antiviral agent netropsin and the structurally related antitrypanosomal drug berenil (Fig. 1).

Several classes of pentamidine analogues have been developed in recent years (11, 12) and, in some cases, there exists a correlation between the DNA binding affinity of the analogues and their anti-PCP activity in rat models (13, 14). Recently, Donkor *et al.* (15) reported the synthesis of a series of four butamidine analogues that proved to be considerably more effective than pentamidine as anti-PCP agents. In these analogues (represented in Fig. 1) the flexible pentamethylene linker between the two amidinophenoxy groups of pentamidine has been replaced by a *cis*- (compounds **4** and **6**) or *trans*- (compounds **5** and **7**) 1,4-but-2-ene chain, i.e., a shorter and more rigid linker. Moreover, in compounds **6** and **7** the amidine termini of pentamidine have been replaced with imidazolidine groups. The NMR and X-ray diffraction studies of the pentamidine-DNA complex have revealed that, while the phenylamidine groups engage in contacts with the bases on the floor of the minor groove, the pentamethylene linker lies in van der

This work was supported by grants (to M.J.W.) from the Wellcome Trust, the Cancer Research Campaign, and the Association for International Cancer Research.

[1] Permanent address: Institut de Recherches sur le Cancer, INSERM Unité 124, Place de Verdun, 59045 Lille Cedex, France.

ABBREVIATIONS: PCP, *Pneumocystis carinii* pneumonia; AMV, avian myeloblastosis virus; MPE, methidium propyl-EDTA.

Waals contact with the C4′ and C5′ sugar atoms on the DNA backbone (at the mouth of the groove), rather than contacting the DNA bases accessible only deep within the minor groove. Thus, any modification of the size and the geometry of the connector could well modify the predisposition of the drug to bind to defined AT-rich sequences in DNA. These observations prompted us to investigate the DNA recognition properties of the butamidine analogues. As part of a continuing effort to widen our understanding of molecular aspects of the interaction of low molecular weight ligands with DNA and their biological properties (16), we report a detailed comparative footprinting study on the binding of netropsin, pentamidine, and four butamidine analogues to two DNA restriction fragments having different base pair composition. The results of these investigations, in which we have used both the endonuclease DNase I (EC 3.1.21.1) and the metal complex MPE·Fe(II) as DNA-cleaving agents, provide clear experimental evidence that all six drugs engage selectively in contact with AT-rich sequences in DNA, with the *cis*-isomers being more potent than the *trans*-isomers in recognizing their target sequences. Although no direct relationship between the DNA-binding selectivity and the anti-PCP activity can be established, the present results point to new opportunities for the rational design of sequence-selective DNA minor groove binders based on pentamidine.

Materials and Methods

Drugs. Netropsin and pentamidine were obtained from Serva and Sigma, respectively. The synthesis of the *cis*- and *trans*-butamidine analogues of pentamidine has been reported recently (15). All six drugs tested showed good aqueous solubility (≥10 mM). In the dry state, drugs were stored in a desiccator in the dark at 4° (or at −20° for some

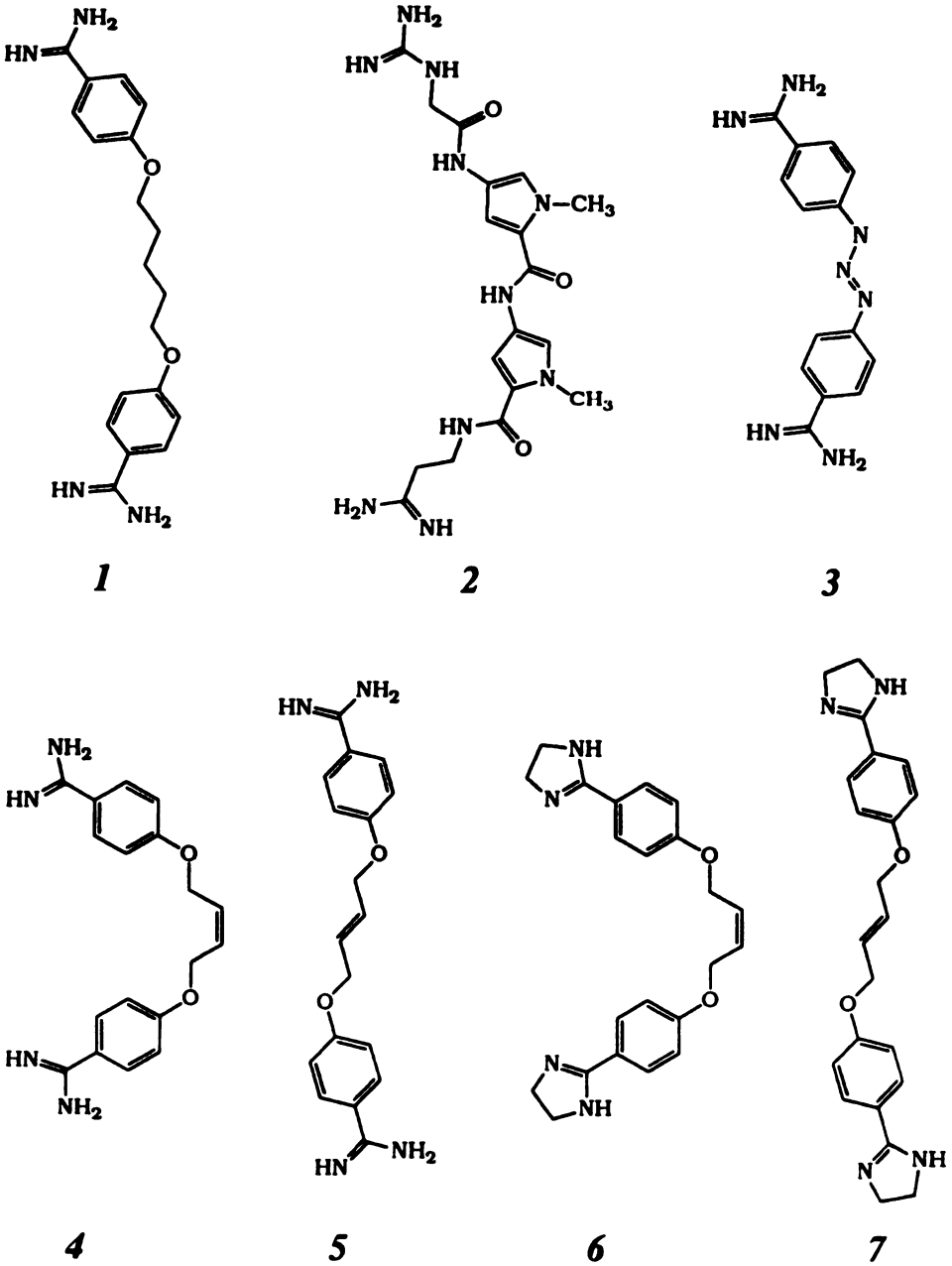

Fig. 1. Chemical structures of pentamidine (1), netropsin (2), berenil (3), and the *cis*- (4 and 6) and *trans*- (5 and 7) butamidine derivatives.

drugs, according to the manufacturer's instructions). Ligand concentrations were determined by direct weighing.

Chemicals and biochemicals. Ammonium persulfate, Tris base, acrylamide, bisacrylamide, ultrapure urea, boric acid, tetramethylethylenediamine, and dimethyl sulfate were from BDH. Formic acid, piperidine, hydrazine, and formamide were from Aldrich. Photographic requisites were from Kodak. Bromophenol blue and xylene cyanol were from Serva. [α-^{32}P]dATP and [γ-^{32}P]ATP were obtained from NEN-DuPont. Unlabeled dATP was ultrapure grade from Pharmacia. Restriction endonucleases *Eco*RI and *Pvu*II (Boehringer, Mannheim, Germany) were used according to the supplier's recommended protocol, in the activity buffer provided. Alkaline phosphatase, T4 polynucleotide kinase, and AMV reverse transcriptase were from Pharmacia. MPE was a gift from Professor Peter Dervan (California Institute of Technology, Pasadena, CA). All other chemicals were analytical-grade reagents, and all solutions were prepared using doubly deionized, filtered (Millipore filters) water.

DNA purification and labeling. Plasmid pBS (Stratagene, La Jolla, CA) was isolated from *Escherichia coli* by a standard sodium dodecyl sulfate-sodium hydroxide lysis procedure and was purified by banding twice in CsCl-ethidium bromide gradients. Ethidium was removed by several isopropanol extractions, followed by exhaustive dialysis against Tris-EDTA buffer. The purified plasmid was then precipitated and resuspended in appropriate buffer before digestion by the restriction enzymes. The two pBS DNA fragments were prepared by 3′-^{32}P-end labeling of the *Eco*RI-*Pvu*II double digest of pBS plasmid using [α-^{32}P]dATP (6000 Ci/mmol) and AMV reverse transcriptase or by 5′-^{32}P-end labeling of the *Eco*RI/alkaline phosphatase-treated pBS plasmid using [γ-^{32}P]ATP (6000 Ci/mmol) and T4 polynucleotide kinase, followed by treatment with *Pvu*II. The 117-mer and 265-mer digestion products were separated on a 6% polyacrylamide gel under native conditions in TBE buffer (89 mM Tris-borate, pH 8.3, 1 mM EDTA). After autoradiography, the band of DNA was excised, crushed, and soaked in elution buffer (500 mM ammonium acetate, 10 mM magnesium acetate) overnight at 37°. This suspension was filtered through a Millipore 0.22-μm filter and the DNA was precipitated with ethanol. After washing with 70% ethanol and vacuum drying of the precipitate, the labeled DNA was resuspended in 10 mM Tris, adjusted to pH 7.0, containing 10 mM NaCl.

DNase I footprinting. DNase I footprinting experiments were performed essentially according to the original protocol (17), as described by Bailly and Waring (18, 19). Reactions were conducted in a total volume of 10 μl. Samples (3 μl) of the labeled DNA fragment were incubated with 5 μl of buffer solution containing the ligand at appropriate concentration. After 30–60 min of incubation at 37° to ensure equilibration of the binding reaction, digestion was initiated by the addition of 2 μl of a DNase I solution whose concentration was adjusted to yield a final enzyme concentration of about 0.01 unit/ml in the reaction mixture. The extent of digestion was limited to <30% of the starting material to minimize the incidence of multiple cuts in any strand ("single-hit" kinetic conditions). Optimal enzyme dilutions were established in preliminary calibration experiments. After 3 min, the digestion was stopped by the addition of 3 μl of an 80% formamide solution containing tracking dyes. Samples were heated at 90° for 4 min and chilled on ice for 4 min before electrophoresis.

MPE footprinting. MPE footprinting was accomplished according to the procedure initially developed by Van Dyke and Dervan (20). Briefly, 2 μl of labeled DNA (approximately 500 cps) were mixed with 5 μl of test ligand at the desired concentration and the drug-DNA complex was left to equilibrate for at least 30 min at 37°. Successively added were 1 μl of MPE (50 μM; aliquots stored at −20°), 1 μl of a freshly prepared 50 μM solution of $Fe(NH_4)_2(SO_4)_2 \cdot 6H_2O$, and then 1 μl of 20 mM dithiothreitol to initiate the cleavage reaction. After 1–5 min of incubation at room temperature, the reaction was stopped by freeze drying. The extent of digestion was again limited to <30% of the starting material. Samples were lyophilized and washed twice with 50 μl of water. The DNA sample was resuspended in 5 μl of formamide-TBE loading buffer, denatured at 90° for 4 min, and then chilled on ice for 4 min before being loaded onto the sequencing gel.

Electrophoresis and autoradiography. DNA cleavage products were resolved by polyacrylamide gel electrophoresis under denaturing conditions (0.3-mm-thick gel, 8% acrylamide containing 8 M urea) capable of resolving DNA fragments differing in length by one nucleotide. Electrophoresis was continued until the bromphenol blue marker had run out of the gel (about 2.5 hr at 60 W and 1600 V in TBE buffer; BRL model S2 sequencer). Gels were soaked in 10% acetic acid for 15 min, transferred to Whatman 3MM paper, dried under vacuum at 80°, and subjected to autoradiography at −70° with an intensifying screen. Exposure times of the X-ray films (Fuji R-X) were adjusted according to the number of counts/lane loaded on each gel (usually 24 hr).

Quantitation by storage phosphor imaging. A Molecular Dynamics 425E PhosphorImager was used to collect data from the storage screens exposed to dried gels overnight at room temperature (21). Baseline-corrected scans were analyzed by integrating all densities between two selected boundaries, using ImageQuant version 3.3 software. Each resolved band was assigned to a particular bond within the pBS fragment by comparison of its position relative to sequencing standards generated by treatment of the DNA with dimethylsulfate (guanine), formic acid (guanine plus adenine), or hydrazine (thymine plus cytosine), followed by piperidine-induced cleavage at the modified bases in DNA.

Results

We began the footprinting studies by investigating the effects of the pentamidine analogues on the cleavage of DNA by the endonuclease DNase I. This enzyme has been extensively used in our laboratory over many years for mapping the DNA binding sites of a large variety of drugs exhibiting antimicrobial, antiviral, and antitumor properties (16, 18, 19). Two different DNA restriction fragments, isolated from the plasmid pBS and 3′- or 5′-end labeled on one or the other of the complementary strands, were used as substrates for DNase I, to visualize at nucleotide resolution the position and length of individual drug binding sites. A typical autoradiograph of a sequencing gel used to fractionate the products of partial digestion of the DNA complexed with the drugs is presented in Fig. 2. In this gel, corresponding to the 117-mer DNA fragment, the DNase I digestion patterns obtained in the absence and presence of the four analogues (compounds **4**-**7**) are compared to those produced with the reference drugs pentamidine (compound **1**) and netropsin (compound **2**). It is immediately apparent that all six compounds hinder to various degrees the cutting of the DNA by the nuclease. Netropsin is the most potent inhibitor of DNA cleavage and generates full gaps in the gel, which reflect complete inhibition of the cutting at defined DNA sequences. The footprinting patterns observed with netropsin are identical to those previously reported with this minor groove-binding agent using the same DNA fragments (22). Although less effective than netropsin, pentamidine and its congeners also inhibit the access of the enzymic probe. The cleavage of the 5′-labeled 117-mer fragment by DNase I is clearly reduced around nucleotide positions 46, 67, and 88. It can also be seen on this autoradiograph that the *trans*-isomers are less efficient than the *cis*-isomers at inhibiting the nuclease activity. Indeed, with compounds **5** and **7** a concentration of 25 μM is required to detect significant cleavage inhibition, whereas 5 μM levels of compounds **4** and **6** are sufficient to produce marked footprints. To compare the effectiveness of the drugs on a more quantitative basis, the band intensities in selected gel lanes from the computerized image of the gels

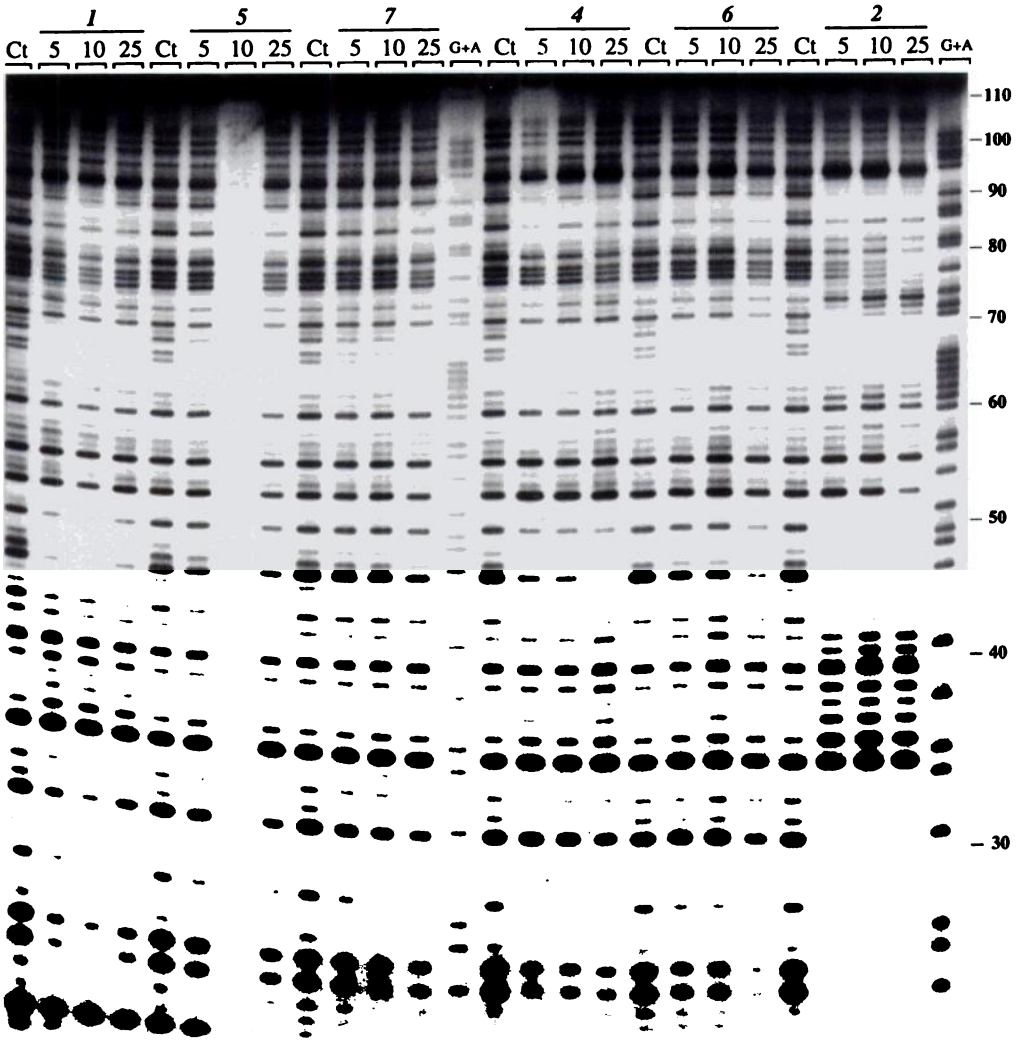

Fig. 2. DNase I footprinting of pentamidine (**1**), netropsin (**2**), and the *cis*- (**4** and **6**) and *trans*- (**5** and **7**) butamidine derivatives with the 117-base pair *Eco*RI/*Pvu*II restriction fragment cut from plasmid pBS. The duplex DNA was 5′-end labeled at the *Eco*RI site with [γ-^{32}P]ATP in the presence of T4 polynucleotide kinase. The cleavage products of the DNase I digestion were resolved on an 8% polyacrylamide gel containing 8 M urea. The concentration (in μM) of the drugs is shown at the top of the appropriate gel lanes. The track corresponding to 10 μM compound **5** is missing. Control (*Ct*) tracks contained no drug. *G+A*, formic acid-piperidine marker specific for purines. *Numbers at the side of the gels* refer to the numbering scheme used in Fig. 3.

displayed on the PhosphorImager were measured. Figs. 3 and 4 show the resulting differential cleavage plots for compounds **1** and **4**-**7** (the plots for netropsin were omitted for clarity). These plots were generated at a common drug concentration of 25 μM for the 117-mer and 5 μM for the 265-mer DNA fragments. Pentamidine and its four analogues produce comparable cutting motifs, indicating that they bind selectively to the same sequences in DNA. However, the amplitude of the inhibition (negative values) or enhancement (positive values) is quite distinct for each drug. The 3′ offset of the DNase I footprints across the two strands of the duplex is in accord with the model for asymmetric cleavage by DNase I across the minor groove of the B-form helix (23). Consistently on both strands of the two DNA fragments, we observed that the *trans*-isomers produced weaker inhibition of DNA cleavage than did the *cis*-isomers. The plots also reveal that the footprints generated by compound **4** are almost always more pronounced than those obtained with compound **6**. Although less obvious, the same observation seems to pertain to the behavior of compound **5**, which produces slightly stronger footprints than does its co-isomeric analogue **7**. Therefore, we can tentatively conclude that the amidine group found in compounds **4** and **5** provides a better anchorage to DNA than does the imidazolidine group present in compounds **6** and **7**. By comparing the intensities of the footprints observed with the 117-mer fragment, we note that the compounds rank in the order **4** $\geq$ **1** > **6** > **5** = **7**.

Five and four major sites of drug protection can be identified on the 117-mer and 265-mer DNA fragments, respectively. Additional drug binding sites can be discerned at the top of the gels but they lie beyond the region accessible to densitometric analysis. The sequences protected from cleavage by the most potent pentamidine derivative, compound **4**, are listed in Table 1, and clearly all nine of these drug-protected regions are situated in AT-rich sequences of the DNA. Adjoining these protected sites are a few regions where the DNase I cutting rate has been substantially enhanced, relative to the control. The cleavage enhancements occur in GC-rich regions such as the sequences 5′-GGCCG (residues 34–38) on the 117-mer and

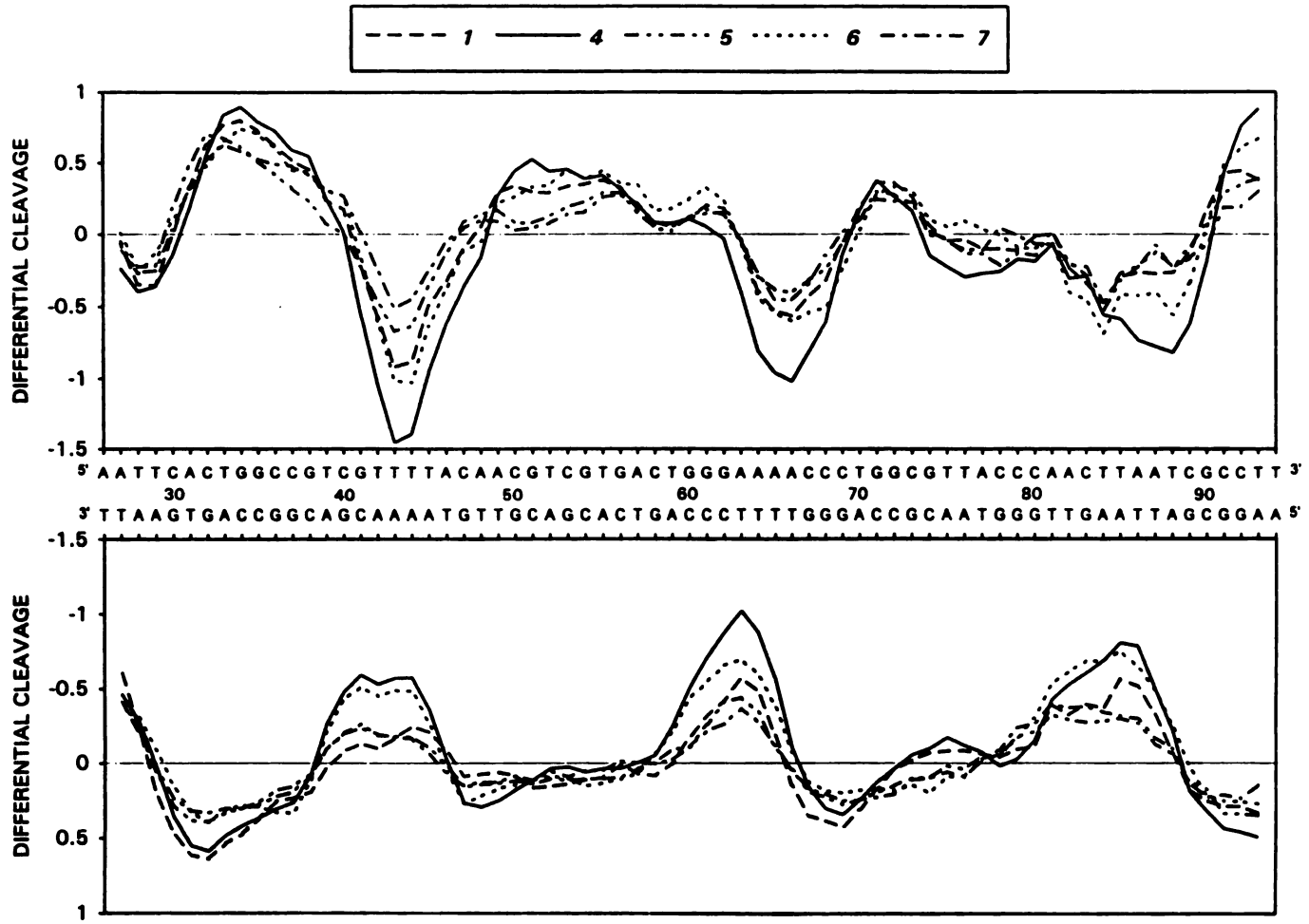

Fig. 3. Differential cleavage plots comparing the susceptibility of the 117-mer DNA fragment to DNase I cutting in the presence of pentamidine and the four butamidine analogues (25 μM each). *Upper*, differential cleavage of the 5′-end-labeled strand; *lower*, cleavage of the complementary 3′-end-labeled strand. The *ordinate scales* for the two strands are inverted, so that deviation of the points toward the lettered sequence (negative values) corresponds to a ligand-protected site and deviation away (positive values) represents enhanced cleavage. *Ordinate scales* are in units of $\ln(f_a) - \ln(f_c)$, where f_a is the fractional cleavage at any bond in the presence of the drug and f_c is the fractional cleavage of the same bond in the control, given closely similar extents of overall digestion. Each *line* drawn represents a 3-bond running average of individual data points, calculated by averaging the value of $\ln(f_a) - \ln(f_c)$ at any bond with those of its two nearest neighbors.

5′-GCAGGC (residues 39–44) on the 265-mer. It is likely that these tracts of moderately enhanced cleavage occur primarily as a result of the mass-action effect described by Goodisman and Dabrowiak (24), rather than as a consequence of conformational changes induced in the DNA by binding of the drugs to neighboring sites, because pentamidine is believed to introduce only minimal distortion into the double helix structure (6).

Consistently on both fragments we note that, the longer the AT tract, the higher the amplitude of the protected cleavage. The most intense footprint is detected around nucleotide 77 on the 265-mer, which corresponds to a run of 7 consecutive A·T base pairs. Taking into account the mechanism of DNase I binding to DNA, and in particular the phosphate residues contacted by the enzyme (23), it is possible to define with some accuracy the sites of drug binding. Considerations such as the 3′ stagger introduced by the enzyme upon DNA cleavage led us to estimate the size of the drug binding sites as varying from 3 to 5 base pairs. A longer site of about 8 base pairs is observed from position 21 to position 29 on the 117-mer fragment (Table 1) but this site, found in the sequence 5′-ATTTACAATT, must correspond to the juxtaposition of two sites, each being 4 base pairs in length. Nearly all binding sites encompass at least 4 contiguous A·T base pairs. The only site that contains just 3 A·T base pairs is situated at position 76 on the 117-mer fragment. However, we note that the DNase I cutting at this site is not reduced by the *trans*-analogues, and with pentamidine and the *cis*-analogues it is inhibited to a much smaller degree, compared with the inhibition occurring at longer AT sequences. Although one must admit that DNase I is not usually sufficiently stringent a probe to define accurately the minimal extent of a binding site for a minor groove binder, it is plausible that the minimal binding site for pentamidine and its analogues may be constituted by 3 A·T base pairs. Such a conclusion appears even more likely given that the related minor groove binder 4′,6-diamidino-2-phenylindole was recently shown to bind selectively in the minor groove of DNA at regions containing only 2 A·T base pairs (25). However, the 3-base pair secondary site at position 76 on the 117-mer is not detected when MPE·Fe(II) is used as a probe (see below), so the safe conclusion is that sequences of 4 consecutive A·T base pairs provide privileged binding sites for both the *cis*- and *trans*-

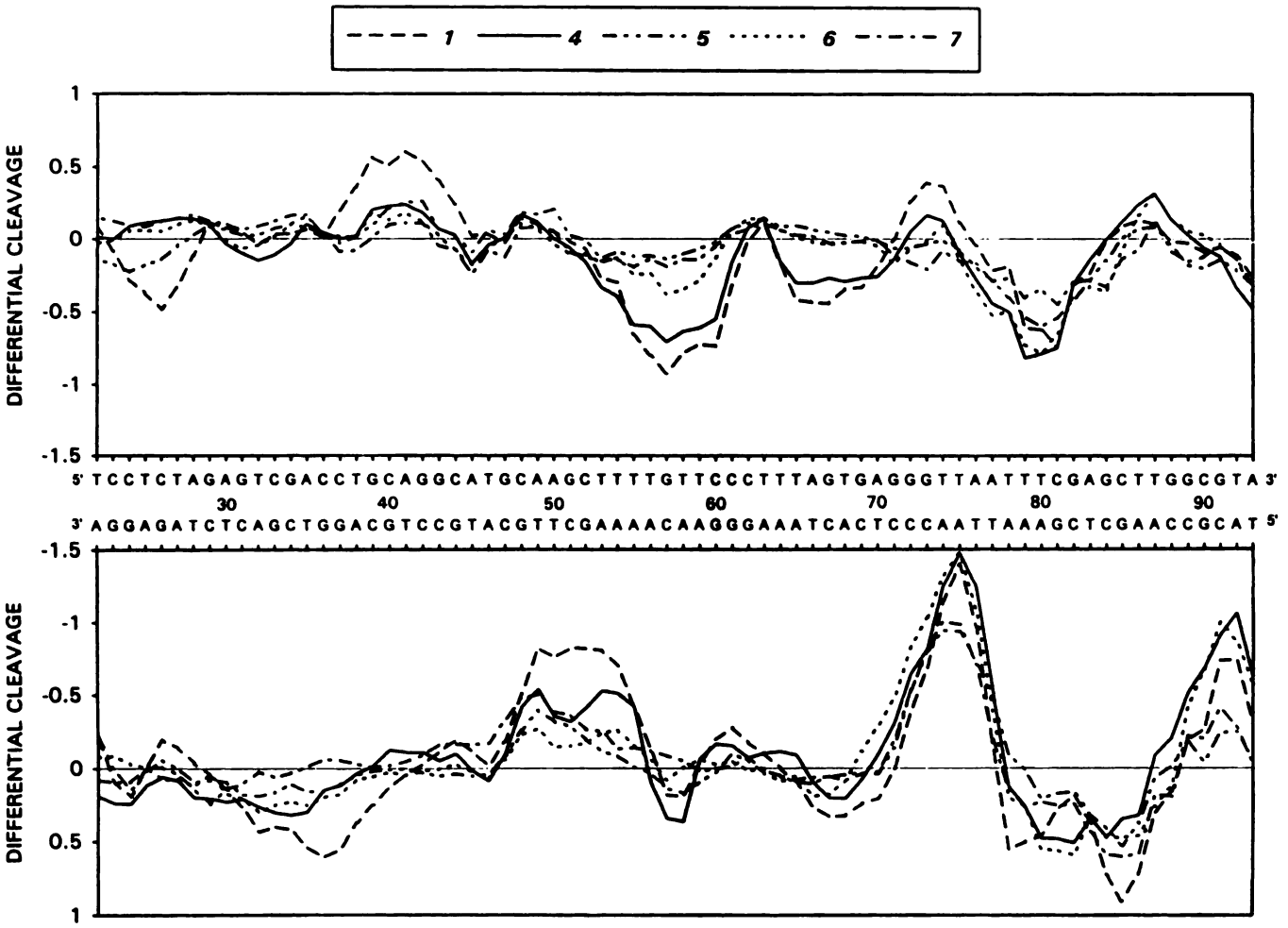

Fig. 4. Differential cleavage plots comparing the susceptibility of the 265-mer DNA fragment to DNase I cutting in the presence of pentamidine and the four butamidine analogues (5 μM each). Other details were as for Fig. 3.

TABLE 1

Sequences in the DNA fragments from plasmid pBS that experience protection from cleavage by DNase I in the presence of the *cis*-analogue 4, inferred from differential cleavage plots

The location of each sequence, with reference to the numbering schemes in Figs. 3 and 4, is indicated in parentheses.

DNA	Protected sequences
117-mer	5′-ATTTACAATT (21–29)
	3′-TAAATGTTA (21–28)
	5′- GTTTTAC (41–47)
	3′-AGCAAAA (39–45)
	5′- AAAACC (63–68)
	3′-ACCCTTTT (59–66)
	5′- GTTACC (74–79)
	3′-GCAAT (73–77)
	5′- ACTTAATC (82–89)
	3′-TTGAATTA (81–88)
265-mer	5′- TTTTGTTC (53–60)
	3′-TCGAAA (50–56)
	5′- TTTAGTGA (63–70)
	3′-GGAAAT (61–66)
	5′- TAATTTCG (75–82)
	3′-CAATTA (73–78)
	5′- TAATCAT (92–98)
	3′-GCATT (90–94)

isomers. These observations correlate satisfactorily with the results of the molecular dynamics and X-ray diffraction studies on the interaction between pentamidine and the *Eco*RI dodecamer d(CGCGAATTCGCG) (6, 10), as well as with previous footprinting studies (8). The results also agree with a recent study on propamidine, a short chain homologue of pentamidine, which was shown to bind to a 4-base pair AT sequence (26).

It is interesting to note that relatively weak inhibition of DNase I cleavage is observed at the sequence 5′-TTTA·3′-AAAT on the 265-mer (positions 63–66), whereas the footprints are significantly more pronounced at the sequences 5′-TTAA or 5′-TTTT (e.g., positions 42–45 and 84–87 on the 117-mer). On the other hand, recent NMR solution studies of the pentamidine-d(CGCAAATTTGCG)$_2$ complex indicated that the drug occupies the sequence 5′-ATTT, rather than the central 5′-AATT site (7). Consistent with the latter observation, a detailed comparison of the binding of the pentamidine analogues to the sequences 5′-TTTT·3′-AAAA and 5′-TTTA·3′-AAAT confirms the preference of the drug for binding to the homopolymeric sequence, relative to the partially alternating sequence (see below).

Other complementary experiments were performed with MPE·Fe(II) in an effort to probe more precisely the exact nature of the various binding sites. Cleavage of DNA by MPE·

Fe(II), although far less sequence specific than cleavage by DNase I, often gives better definition of each binding site, leading to a more parsimonious estimate of the site size (27). Densitometric analysis of the autoradiograms is, however, mandatory (20).

Cutting patterns produced by MPE·Fe(II) with the 3′-end-labeled strand of the 265-mer fragment in the absence and presence of pentamidine and its analogues are shown in Fig. 5. Regions of attenuated cleavage by MPE·Fe(II) are sufficiently pronounced to be identifiable around nucleotide positions 55, 77, and 92 on this autoradiograph. An example of a gel obtained for one strand of the 117-mer fragment is shown in Fig. 6 and, here again, the footprints can be easily distinguished. The results for both strands of each of the two pBS DNA fragments are summarized in Fig. 7, in the form of protection maps derived from the corresponding differential cleavage plots obtained after quantitative analysis of the phosphorimages. Zones of protection from MPE·Fe(II) attack can be observed in many of the same places as for DNase I (compare with the plots in Figs. 3 and 4). The MPE·Fe(II) footprinting data support the conclusions drawn from the DNase I results regarding the preferential binding sites for all of the ligands and confirm that pentamidine and its analogues bind best to the sequence 5′-TTTT·3′-AAAA. At marginal drug concentrations a footprint can be observed at this tract in the 265-mer fragment before footprints are identifiable at any other AT-rich regions.

From the DNase I footprinting data it appeared clear that the *cis*-analogues produce more pronounced footprints than do the *trans*-analogues. The same observation pertains when MPE·Fe(II) is used, but the difference is less pronounced. The extent of protection against cleavage induced by compounds **4** and **6** is consistently greater than that produced by compounds **5** and **7** at all binding sites amenable to examination (data not shown). A rigorous comparison between the effects of *cis*- and *trans*-isomers is not yet available but could be obtained by a full quantitative footprinting analysis (28). Our best estimate at present is that the relative binding constants for the two isomers differ by a significant factor but <1 order of magnitude.

Discussion

The present results corroborate the findings of a previous footprinting study (8) showing that pentamidine binds selectively to AT-rich sequences in DNA, a preference shared with the four butamidine analogues studied here as well as with several other minor groove binders examined in the past, including berenil, netropsin, distamycin, 4′,6-diamidino-2-phenylindole, and Hoechst 33258 (29, 30). The conclusions regarding the nature of the pentamidine binding sites on DNA are in total agreement with early spectroscopic measurements (31) and with recent X-ray (6) and solution NMR studies (7).

Both the *cis*- and *trans*-analogues of butamidine appear to bind fairly specifically to a run of 4 A·T base pairs. Although on a single occasion a 5′-TTA triplet appeared to serve as a weak binding site [inferred from the DNase I footprinting plots but not seen by using MPE·Fe(II)], it seems that 3-base pair sequences are generally not sufficient to satisfy the butamidine-DNA recognition process. The footprinting data also reveal that isolated G·C base pairs are not tolerated within a binding site. It is evident from a close inspection of Figs. 2–7 that major differences exist between the four analogues regarding the extent to which any particular AT binding sequence is protected

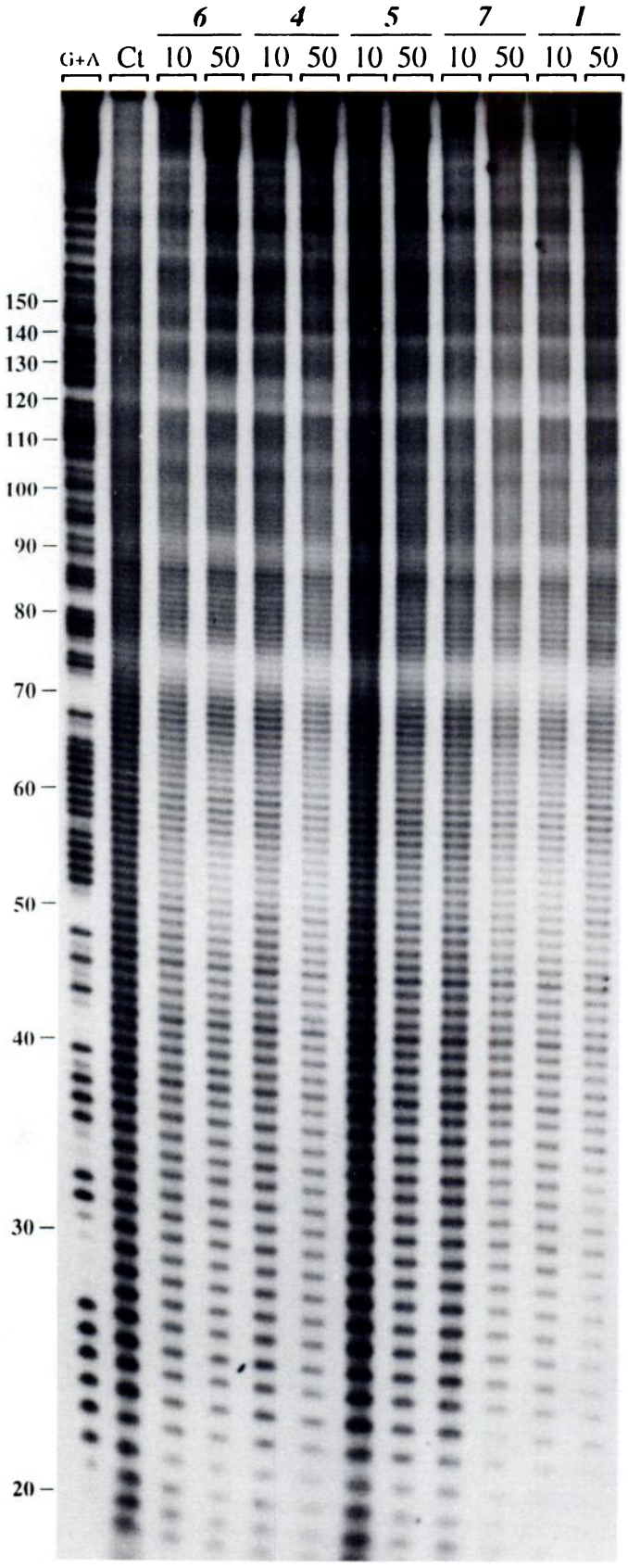

Fig. 5. MPE·Fe(II) footprinting of pentamidine (**1**) and the *cis*- (**4** and **6**) and *trans*- (**5** and **7**) butamidine analogues with the 265-mer. The duplex DNA was 3′-end labeled at the *Eco*RI site with [α-^{32}P]dATP in the presence of AMV reverse transcriptase. Other details were as for Fig. 2.

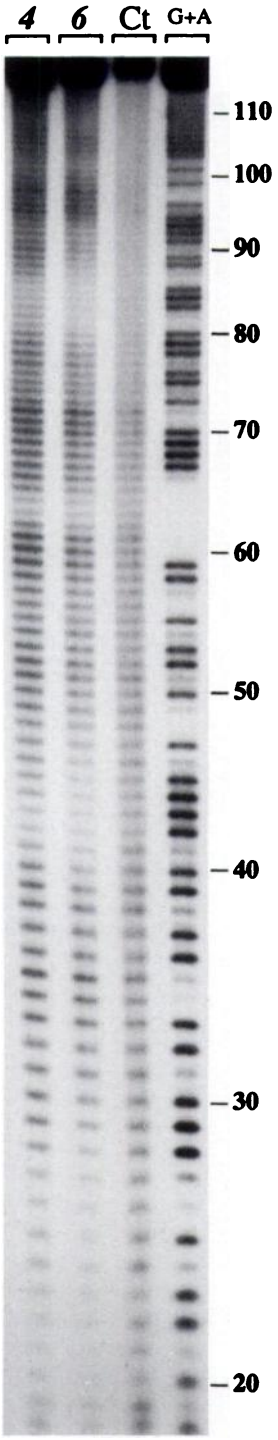

Fig. 6. MPE·Fe(II) footprinting of the *cis*-butamidine derivatives **4** and **6** with the 3′-end-labeled 117-mer fragment from pBS. Other details were as for Figs. 2 and 5.

against cleavage. In other words, both the chemical structure of the positively charged terminal groups and the geometry of the but-2-ene connector appear to play determining roles in allowing the drug to engage in contacts with DNA.

In terms of structure-DNA binding relationships, several pertinent conclusions emerge from the present footprinting data. Compound **4** generates stronger footprints than does its analogue **6**. Because these two *cis*-derivatives differ only in the nature of their terminal groups, the results suggest that the amidine groups provide a better anchorage into DNA than do the imidazolidine groups. The replacement of the amidine function by the imidazolidine moiety, which is considerably larger than the amidine group, results in a slight decrease of the extent of binding but does not modify the AT-specific DNA recognition process. We note that these observations are not entirely consistent with previous studies showing that cyclization of the amidine group into the imidazolidine group has no influence on the DNA binding affinity of pentamidine analogues (14). Our data provide an interesting comparison with those of Wilson *et al.* (32), who compared the binding properties of a series of diphenylfuran derivatives containing amidine or imidazolidine terminal groups. The footprinting data reported here are at variance, although not seriously, with their conclusion that "the extra size and reduced hydrogen bonding capacity of the imidazolidine group relative to the amidine are not detrimental to complex formation at AT minor groove sites" (32, page 349).

The *cis*-isomers **4** and **6** produce clearer footprints than do the *trans*-isomers **5** and **7**. At first sight, we thought that the replacement of the flexible pentamethylene chain of pentamidine with a shorter semi-rigid linker would provide tighter anchorage into DNA. It is clear that this is not necessarily true; the conformation of the linker is critical. The amidine (**4** and **5**) and imidazolidine (**6** and **7**) derivatives have similar hydrogen-bonding potentialities but they have distinct molecular shapes, which apparently constitute an element of prime importance in favoring (*cis*-conformation) or hampering (*trans*-conformation) the fitting of the drugs into the minor groove of DNA. The observation that the *cis*-analogues exhibit superior DNA recognition capacities, compared with the *trans*-analogues, is extremely interesting. At the outset of this work, considering the notion of DNA isohelicity (33), we expected that the *trans* geometry would prove favorable. The phasing problem in ligand-DNA interactions has been carefully addressed via the development of bis-netropsin derivatives connected by *cis*- and *trans*-linkers (34). Bidentate binding at $(AT)_n$ sequences was shown to occur when the two DNA-reading elements are connected by *trans*-olefinic or *trans*-cycloalkane linkers, whereas compounds equipped with *cis*-linkers exhibit monodentate binding (35, 36). The present results reveal the opposite situation; the *cis*-isomers fit better into AT sites than do the *trans*-homologues. Thus, these results appear at odds with a sound precedent. However, careful consideration of several studies on pentamidine and its analogues can resolve the apparent discrepancy. Neidle and co-workers (26) have recently shown that propamidine binds more strongly to DNA than does pentamidine and in addition, despite their chemical homology, these two compounds differently affect the width of the minor groove, which is known to be a dominant factor determining drug-DNA recognition (37). The *cis*-analogues **4** and **6** are shorter than the *trans*-analogues **5** and **7**, and that factor by itself might contribute to their easier complexation with DNA. However, we believe that the critical findings that support the validity of our footprinting data come from two recent molecular modeling analyses of the binding to DNA of a series of pentamidine analogues differing in the length of the hydrocarbon connector and in the positioning of the amidinium ends on the phenoxy rings. First, Cory *et al.* (14) have reported a correlation between the DNA binding affinity and the radius of curvature of molecular models for 39

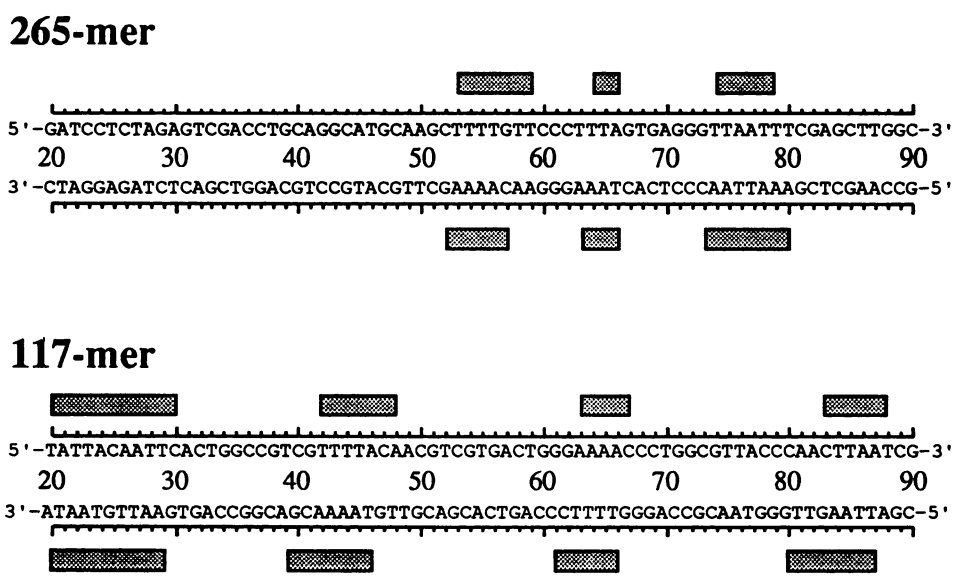

Fig. 7. Summary map representing the MPE·Fe(II) footprints detected with the *cis*-butamidine derivative **4** on both strands of the 265- and 117-base pair *Eco*RI-*Pvu*II restriction fragments from plasmid pBS. Only the region of each restriction fragment analyzed by densitometry is shown. *Dotted boxes*, positions of inhibition of MPE·Fe(II) cutting in the presence of compound **4** (presumptive binding sites inferred from differential cleavage plots). *Upper* and *lower footprints* are from 5′- and 3′-end-labeled DNA, respectively. Data were compiled from quantitative analysis of several sequencing gels and must be considered as a set of averaged values.

analogues of pentamidine. According to their computations, a molecule having a radius of curvature close to that of the target sequence exhibits a higher affinity for DNA than does a molecule with a radius of curvature larger than that of the minor groove. It seems evident that the linearly organized *trans*-analogues **5** and **7** would exhibit much larger radii of curvature than the highly curved *cis*-analogues **4** and **6** (Fig. 1). Therefore, based on reasoning analogous to that used by Cory *et al.* (14), we can rationalize the different capacities of the *cis*- and *trans*-analogues of butamidine to recognize defined DNA sequences in terms of the respective molecular shapes of these drugs. The second computational study (10) indicates that *meta* placement of the amidinium groups should facilitate effective penetration into the DNA minor groove for analogues containing even numbers of carbon atoms (e.g., for butamidine analogues). In contrast, for compounds with an odd number of carbon atoms in the linker the *para*-substituted bis(amidine) arrangement is predicted to be more isohelical with the minor groove of DNA. Although the four butamidine analogues studied here all bear *para*-amidine groups, in terms of overall drug shape it is reasonable to liken the *trans*-analogue **5** and the *cis*-analogue **4** to butamidine [1,4-bis(4-amidinophenoxy)butane] and its *meta* homologue [1,4-bis(3-amidinophenoxy)butane], respectively. For both the latter *meta*-butamidine derivative and the *cis*-compound **4**, the distance between the two terminal amidine groups is shorter than the distance separating the amidine groups in butamidine and the *trans*-analogue **5**. Given these structural analogies and assuming that the theoretical predictions are correct, it is entirely logical that the *cis*-compounds should fit more snugly into the narrow minor groove of an AT tract, compared with the *trans*-compounds. By analogy with the energy-minimized models for the butamidine-d(CGCGAATTCGCG)$_2$ complex (10), it is tempting to postulate that the *trans*-analogues make hydrogen-bonded contacts with the deoxyribose acceptor atoms (as for pentamidine), whereas the *cis*-analogues achieve superior contacts by hydrogen-bonding directly to the DNA bases on the floor of the minor groove. Thus, the computer models indirectly lend credence to our experimental observations, but of course further work will be required to confirm or reject the proposed structural analogies.

On the basis of the footprinting data reported here, we can begin to address the question of whether the DNA sequence selectivity of pentamidine analogues can be related to their biological activity. The butamidine analogues **4**-**7** have been evaluated for anti-PCP activity in rat models (14). All four analogues proved to be more effective than pentamidine in treating *Pneumocystis carinii* infection. The *trans*-bis(amidino) derivative **5** is >5 times more active than pentamidine. In terms of anti-PCP activity, the test molecules rank in the order $\mathbf{5} > \mathbf{4} = \mathbf{6} = \mathbf{7} \gg \mathbf{1}$, whereas in terms of DNA recognition the ranking order is $\mathbf{4} \geq \mathbf{1} \geq \mathbf{6} > \mathbf{5} = \mathbf{7}$. Therefore, with the present data the AT-specific DNA recognition by this series of butamidine derivatives cannot be correlated with their potency against PCP.

This is not the only recent study that has failed to find a correlation between the DNA-binding properties of pentamidine analogues and their effectiveness against PCP (13). Accordingly, if binding to DNA plays an important (or essential) part in the biological activity of pentamidine and its analogues, then their anti-PCP effect must demand more than specific complex formation between the drugs and AT sequences in DNA, perhaps implicating the involvement of a third species such as a nuclear protein. On this basis two hypotheses built around the idea of ancillary DNA-related factors are worth considering. First, it is perfectly plausible to suggest that pentamidine can inhibit the binding of nuclear proteins such as transcription factors to specific target gene sequences containing AT-rich tracts. Such an effect has already been reported for the structurally related AT-specific minor groove binder distamycin (5, 38, 39). The second hypothesis derives from the remarkable ability of $(A)_n \cdot (T)_n$ sequences (i.e., the preferred targets in duplex DNA for pentamidine and its butamidine analogues) to form triple helices with a third AT-rich strand in the major groove of the helix (40). One may conceive that the present drugs could operate by modulating, either positively or negatively, the propensity of their target sequences to engage in triple helix formation *in vivo*. The aforementioned antiviral antibiotic distamycin is known to be capable of binding to triple

helices (41). We intend to investigate the interaction of pentamidine and its congeners with triple-stranded structures to seek evidence of correlation with biological activity.

Acknowledgments

C.B. thanks the INSERM.

References

1. Montgomery, A. B., J. M. Luce, J. Turner, E. T. Lin, R. J. Debs, K. J. Corkery, E. N. Brunette, and P. C. Hopewell. Aerosolised pentamidine as sole therapy for *Pneumocystis carinii* pneumonia in patients with acquired immunodeficiency syndrome. *Lancet* **2**:480–482 (1987).
2. Gazzard, B. G. *Pneumocystis carinii* pneumonia and its treatment in patients with AIDS. *J. Antimicrob. Chemother.* **23**:67–75 (1989).
3. Wispelwey, B., and R. D. Pearson. Pentamidine: a review. *Infect. Control Hosp. Epidemiol.* **12**:375–381 (1991).
4. Grmek, M. D. *History of AIDS: Emergence and Origin of a Modern Pandemic.* Princeton University Press, Princeton, NJ (1990).
5. Gambari, R., and C. Nastruzzi. DNA-binding activity and biological effects of aromatic polyamidines. *Biochem. Pharmacol.* **47**:599–610 (1994).
6. Edwards, K. J., T. C. Jenkins, and S. Neidle. Crystal structure of a pentamidine-oligonucleotide complex: implications for DNA-binding properties. *Biochemistry* **31**:7104–7109 (1992).
7. Jenkins, T. C., A. N. Lane, S. Neidle, and D. G. Brown. NMR and molecular modeling studies of the interaction of berenil and pentamidine with $d(CGCAAATTTGCG)_2$. *Eur. J. Biochem.* **213**:1175–1184 (1993).
8. Fox, K. R., C. E. Sansom, and M. F. G. Stevens. Footprinting studies on the sequence-selective binding of pentamidine to DNA. *FEBS Lett.* **266**:150–154 (1990).
9. Sansom, C. E., C. A. Laughton, S. Neidle, C. H. Schwalbe, and M. F. G. Stevens. Structural studies on bio-active compounds. XIV. Molecular modelling of the interactions between pentamidine and DNA. *Anti-Cancer Drug Design* **5**:243–248 (1990).
10. Greenidge, P. A., T. C. Jenkins, and S. Neidle. DNA minor groove recognition properties of pentamidine and its analogs: a molecular modeling study. *Mol. Pharmacol.* **43**:982–988 (1993).
11. Walzer, P. D., C. K. Kim, J. Foy, M. J. Linke, and M. Cushion. Cationic antitrypanosomal and other antimicrobial agents in the therapy of experimental *Pneumocystis carinii* pneumonia. *Antimicrob. Agents Chemother.* **32**:896–905 (1988).
12. Jones, S. K., J. E. Hall, M. A. Allen, S. D. Morrison, K. A. Ohemeng, V. V. Reddy, J. G. Geratz, and R. R. Tidwell. Pentamidine analogs in the treatment of experimental *Pneumocystis carinii* pneumonia. *Antimicrob. Agents Chemother.* **34**:1026–1030 (1990).
13. Tidwell, R. R., J. D. Jones, J. D. Geratz, K. A. Ohemeng, M. Cory, and J. E. Hall. Analogues of 1,5-bis(4-aminophenoxy)pentane (pentamidine) in the treatment of experimental *Pneumocystis carinii* pneumonia. *J. Med. Chem.* **33**:1252–1257 (1990).
14. Cory, M., R. R. Tidwell, and T. A. Fairley. Structure and DNA binding activity of analogues of 1,5-bis(4-aminophenoxy)pentane (pentamidine). *J. Med. Chem.* **35**:431–438 (1992).
15. Donkor, I. O., S. K. Jones, and R. R. Tidwell. Pentamidine congeners. 1. Synthesis of *cis*- and *trans*-butamidine analogues as anti-*Pneumocystis carinii* pneumonia agents. *Bioorg. Med. Chem. Lett.* **3**:1137–1140 (1993).
16. Waring, M. J., and C. Bailly. DNA recognition by intercalators and hybrid molecules. *J. Mol. Recognition*, in press.
17. Low, C. M. L., H. R. Drew, and M. J. Waring. Sequence-specific binding of echinomycin to DNA: evidence for conformational changes affecting flanking sequences. *Nucleic Acids Res.* **12**:4865–4877 (1984).
18. Bailly, C., and M. J. Waring. Footprinting studies on the sequence-selective binding of tilorone to DNA. *Antiviral Chem. Chemother.* **4**:113–126 (1993).
19. Bailly, C., and M. J. Waring. Preferential intercalation at AT sequences in DNA by lucanthone, hycanthone, and indazole analogs: a footprinting study. *Biochemistry* **32**:5985–5993 (1993).
20. Van Dyke, M. W., and P. B. Dervan. Methidium propyl-EDTA·Fe(II) and DNAase I footprinting report different small molecule binding site sizes on DNA. *Nucleic Acids Res.* **11**:5555–5567 (1983).
21. Johnston, R. F., S. C. Pickett, and D. L. Barker. Autoradiography using storage phosphor technology. *Electrophoresis* **11**:355–360 (1990).
22. Bailly, C., P. Colson, C. Houssier, R. Houssin, D. Mrani, G. Gosselin, J. L. Imbach, M. J. Waring, J. W. Lown, and J. P. Hénichart. Binding properties and DNA sequence-specific recognition of two bithiazole-linked netropsin hybrid molecules. *Biochemistry* **31**:8349–8362 (1992).
23. Weston, S. A., A. Lahm, and D. Suck. X-ray structure of the DNase I-$d(GGTATACC)_2$ complex at 2.3 Å resolution. *J. Mol. Biol.* **226**:1237–1256 (1992).
24. Goodisman, J., and J. C. Dabrowiak. Structural changes and enhancements in DNase I footprinting experiments. *Biochemistry* **31**:1058–1064 (1992).
25. Trotta, E., E. D'Ambrosio, N. Del Grosso, G. Ravagnan, M. Cirilli, and M. Paci. ^1H NMR study of $[d(GCGATCGC)]_2$ and its interaction with minor groove binding 4′,6-diamidino-2-phenylindole. *J. Biol. Chem.* **268**:3944–3951 (1993).
26. Nunn, C. M., T. C. Jenkins, and S. Neidle. Crystal structure of d(CGCGAATTCGCG) complexed with propamidine, a short-chain homologue of the drug pentamidine. *Biochemistry* **32**:13838–13843 (1993).
27. Dabrowiak, J. C., K. Kissinger, and J. Goodisman. Quantitative footprinting analysis od drug-DNA interactions: Fe(III) methidium-propyl-EDTA as a probe. *Electrophoresis* **10**:404–412 (1989).
28. Dabrowiak, J. C., and J. Goodisman. Quantitative footprinting analysis of drug-DNA interactions, in *Chemistry and Physics of DNA-Ligand Interactions* (N. R. Kallenbach, ed.). Adenine Press, Guilderland, New York, 143–174 (1989).
29. Portugal, J., and M. J. Waring. Comparison of the binding sites for berenil, netropsin and distamycin. *Eur. J. Biochem.* **167**:281–289 (1987).
30. Portugal, J., and M. J. Waring. Assignment of DNA binding sites for 4′,6-diamidine-2-phenylindole and bisbenzimide (Hoechst 33258): a comparative footprinting study. *Biochim. Biophys. Acta* **949**:158–168 (1987).
31. Luck, G., C. Zimmer, and D. Schweizer. DNA binding studies of the non intercalative ligand pentamidine: dA-dT base pair preference. *Stud. Biophys.* **125**:107–119 (1988).
32. Wilson, W. D., F. A. Tanious, H. Buczak, M. K. Venkatramanan, B. P. Das, and D. W. Boykin. The effects of ligand structure on binding mode and specificity in the interaction of unfused aromatic cations with DNA, in *Molecular Basis of Specificity in Nucleic Acid-Drug Interactions* (B. Pullman and J. Jortner, eds.). Kluwer Academic Publishers, London, 331–353 (1990).
33. Goodsell, D., and R. E. Dickerson. Isohelical analysis of DNA groove-binding drugs. *J. Med. Chem.* **29**:727–733 (1986).
34. Lown, J. W. Design of sequence-specific agents: lexitropsins, in *Molecular Aspects of Anticancer Drug-DNA Interactions* (S. Neidle and M. J. Waring, eds.), Vol. 2. Macmillan, London, 322–355 (1993).
35. Rao, K. E., J. Zimmermann, and J. W. Lown. Sequence-selective DNA binding by linked bis-*N*-methylpyrrole dipeptides: an analysis by MPE footprinting and force field calculations. *J. Med. Chem.* **56**:786–797 (1991).
36. Wang, W., and J. W. Lown. Anti-HIV-I activity of linked lexitropsins. *J. Med. Chem.* **35**:2890–2897 (1992).
37. Neidle, S. Minor groove width and accessibility in B-DNA drug and protein complexes. *FEBS Lett.* **298**:97–99 (1992).
38. Dorn, A., M. Affolter, M. Muller, W. J. Gehring, and W. Leupin. Distamycin-induced inhibition of the homeodomain-DNA complexes. *EMBO J.* **11**:279–286 (1992).
39. Gambari, R., R. Barbieri, C. Nastruzzi, V. Chiorboli, G. Feriotto, P. G. Natali, P. Giacomini, and F. Arcamone. Distamycin inhibits the binding of a nuclear factor to the −278/−256 upstream sequence of the human HLA-DRα gene. *Biochem. Pharmacol.* **41**:497–502 (1991).
40. Hélène, C. Rational design of sequence-specific oncogene inhibitors based on antisense and antigene oligonucleotides. *Eur. J. Cancer* **27**:1466–1471 (1991).
41. Umemoto, K., M. H. Sarma, G. Gupta, J. Luo, and R. H. Sarma. Structure and stability of a DNA triple helix in solution: NMR studies on $d(T)_6 \cdot d(A)_6 \cdot d(T)_6$ and its complex with a minor groove binding drug. *J. Am. Chem. Soc.* **112**:4539–4545 (1990).

Send reprint requests to: Michael J. Waring, Department of Pharmacology, University of Cambridge, Tennis Court Road, Cambridge CB2 1QJ, UK.